

Possible origins of resistive tails and critical currents in high-temperature superconductors in a magnetic field

D. H. Kim, K. E. Gray, R. T. Kampwirth, and D. M. McKay

Materials Science Division, Argonne National Laboratory, Argonne, Illinois 60439

(Received 9 April 1990)

The universal lack of a Lorentz-force dependence on dissipation for fields parallel to the CuO_2 planes of the highly anisotropic high-temperature superconductor $\text{Tl}_2\text{Ba}_2\text{CaCu}_2\text{O}_x$ questions whether flux motion is the cause of this dissipation. We report measurements over a wide range of current densities, in the broadened resistive transitions, current-voltage characteristics $I(V)$, and critical current densities J_c . We rule out the suggestion that this effect is caused by vortices in the CuO_2 planes, due to a small misalignment of fields parallel to these planes: That model requires a significantly larger field component perpendicular to the planes than is reasonable, based on the measured alignment of the samples and crystal axes. Instead, we consider a Josephson-coupling model that is consistent with the broadened resistive transitions and the lack of Lorentz-force dependence. A detailed comparison of the predictions of these models is made: The Josephson-coupling model is consistent with the temperature dependences of the activation energy U and J_c , and is better matched to the weak-field dependence of J_c ; while the flux-creep model fits the experimental result for U , but it predicts a much stronger temperature and field dependence of J_c than is found. Possible origins of Josephson junctions in high-quality films and single crystals are discussed. For the data with the field parallel to the c axis, a conventional flux-flow explanation is also quite reasonable.

I. INTRODUCTION

The broadened resistive transitions of high-temperature superconductors (HTS) in a magnetic field H parallel to the CuO_2 phase have been shown¹⁻⁴ to be independent of the macroscopic Lorentz force in the highly anisotropic HTS, $\text{Bi}_2\text{Sr}_2\text{CaCu}_2\text{O}_x$, $\text{Tl}_2\text{Ba}_2\text{CaCu}_2\text{O}_x$, and recently² in $\text{YBa}_2\text{Cu}_4\text{O}_8$. Since the Lorentz force is essential to understand such losses in terms of magnetic-flux motion, these authors have questioned this commonly held belief. Others have made various attempts to reconcile this contradiction. Explanations based on flux cutting⁵ or deviations of the microscopic current from its macroscopic direction (thus allowing a microscopic Lorentz force and flux motion) cannot explain the virtual equivalence of the results for the current perpendicular and parallel to the field direction. The role of the extremely high anisotropy of the field-dependent properties of HTS has also been discussed widely: recently, Kes *et al.*⁶ argued that only the component of the field H_\perp that is perpendicular to the CuO_2 conducting planes gives rise to a vortex lattice, and that the zeros in the order parameter and screening currents are restricted to these planes. They claim that such a model can explain: (a) the variation of the broadened resistive transition as a function of the angle between the c axis and the field; (b) the variation of critical current density, J_c , determined from magnetization measurements for fields that are parallel (\parallel) and perpendicular (\perp) to the CuO_2 conducting planes; and (c) the magnetic torque, τ , as a function of angle, ϕ , between H and the c axis. However, these interpretations can be understood simply by decomposing the

applied field into $H_\perp = H \cos\phi$, and a sufficiently large anisotropy (≥ 20) of the field-dependent resistivity, for (a); the reasonable assumption that J_c depends predominantly on H_\perp , for (b); and the highly anisotropic upper critical field, H_{c2} , for (c), although (c) is contradicted by recent torque experiments.⁷ Of greater importance for the present study, these considerations say *nothing* about whether J_c and/or the resistive dissipations are due to flux motion.

In addition, Kes *et al.*⁶ suggest that H_\perp can explain the resistive dissipation as due to flux motion for $\mathbf{H}\parallel\mathbf{a}$ without any Lorentz-force dependence. They correctly point out that when aligning H perpendicular to the c axis, i.e., $\mathbf{H}\parallel\mathbf{a}$, where \mathbf{a} lies in the CuO_2 conducting planes, the required angular tolerance would be too great to avoid some finite H_\perp even for the best single crystal. But their suggestion requires that the broadened resistive transitions for $\mathbf{H}\parallel\mathbf{a}$ can be scaled to similar transitions for $\mathbf{H}\perp\mathbf{a}$, but at a reduced field, $H_0 = H_\perp$. They were unable to test this prediction with available data. We have made a quantitative test and our results are inconsistent with the above suggestion: In all cases, the values of H_0 are *much* too large to have resulted from the narrow distributions of c -axis misorientation measured by x-ray rocking curves or any possible misalignment of the sample. Thus, the question about the dissipation mechanism is left unanswered.

We have measured the broadened resistive transitions, J_c and the current-voltage characteristics, $I(V)$, in highly oriented films of $\text{Tl}_2\text{Ba}_2\text{CaCu}_2\text{O}_x$ for both orientations of the field with respect to the crystal axes and transport current. New data are also presented for the broadened

resistive transitions in $\text{Bi}_2\text{Sr}_2\text{CaCu}_2\text{O}_x$ single crystals. These measurements span the temperature range from 4.2 to 100 K in fields up to 10 T, and *no significant dependence on the macroscopic Lorentz force is ever found.*

As an alternative to flux motion, we consider a Josephson-coupling model (which is explained in detail in Secs. IV and V) for dissipation which has satisfactorily explained similar results in granular NbN films,⁸ gives a natural explanation of the lack of *any* Lorentz-force dependence and is consistent with the broadened resistive transitions, J_c and $I(V)$. A detailed comparison of the predictions of these models to $\text{Tl}_2\text{Ba}_2\text{CaCu}_2\text{O}_x$ is made: The Josephson-coupling model is consistent with the temperature dependences of J_c and the activation energy, U , and is better matched to the weak-field dependence of J_c , while the flux-creep model fits the experimental result for U , but it predicts a much stronger temperature and field dependence of J_c than is found. Possible origins of Josephson junctions in high-quality films and single crystals are discussed.

It is important to recognize that the $I(V)$ provide the necessary clue to determine whether J_c measurements, made with an appropriate voltage criterion, indicate the dramatic onset of dissipation or just reflect the continuing broadening of the resistive transition with field.

II. SAMPLE PREPARATION AND STRUCTURAL CHARACTERIZATION

Sputtered films of $\text{Tl}_2\text{Ba}_2\text{CaCu}_2\text{O}_x$ were prepared in a three-gun dc magnetron sputtering system.⁹ Three targets of Tl, Cu, and a 1:1 Ba-Cu mixture are simultaneously sputtered in a 20 mtorr Ar atmosphere with an O_2 partial pressure of 4×10^{-5} Torr. The films were deposited onto (100) single-crystalline substrates of MgO, which were kept at 210°C during deposition. The films were wrapped in gold foil together with Tl-Ba-Ca-Cu-O bulk materials and annealed in flowing O_2 at 870°C for 6 min, then slowly cooled at a rate of 10°C/min. Electrical contact was made by sputtering Ag through a mask and lead wires were attached by pressing In dots. Contact resistance was found to be less than 1 Ω at room temperature and negligibly small below T_c . X-ray-diffraction analysis indicated a high degree of orientation of the 2:2:1:2 phase with its c axis perpendicular to the substrate, with the half-width at half maximum (HWHM) of the rocking curve for $\text{Tl}_2\text{Ba}_2\text{CaCu}_2\text{O}_x$ films consistently being $\leq 0.4^\circ$, and for the sample reported here, it was only 0.2° for the (0010) peak. Further evidence for the high degree of c -axis orientation comes from torque magnetization measurements¹⁰ on similarly made thin films, which indicated the HWHM was $\leq 0.35^\circ$. The samples were then sliced to a width of 0.05 cm for J_c measurements.

Single crystals of $\text{Bi}_2\text{Sr}_2\text{CaCu}_2\text{O}_x$ were grown using a flux method.¹¹ Here x-ray diffraction shows the HWHM of the rocking curve for $\text{Bi}_2\text{Sr}_2\text{CaCu}_2\text{O}_x$ single crystals is $\sim 0.6^\circ$ for the (0010) peak. Electrical contact was made with silver paste, but only the resistive tails could be measured due to the high contact resistance.

Resistance, J_c and $I(V)$ measurements were performed

in a ^4He gas-flow cryostat equipped with 13.5-T superconducting solenoid.

III. LORENTZ-FORCE DEPENDENCE AND CRYSTALLINE ANISOTROPY

A. Resistive transitions, $\rho(T, H)$

The resistive transitions for $\text{Tl}_2\text{Ba}_2\text{CaCu}_2\text{O}_x$ films are shown in the Arrhenius plots of Fig. 1 for a current density of 10 A/cm². It is clear that the curves have a similar shape for the magnetic field, H , in both relevant orientations, $H \perp \mathbf{a}$ and $H \parallel \mathbf{a}$, where \mathbf{a} is a vector \perp to c and hence in the CuO_2 plane. Given enough patience, field values could be found to overlap the curves and make a convincing case for the similarity between $H \perp \mathbf{a}$ and $H \parallel \mathbf{a}$. However, from Fig. 1, we estimate that there is ~ 15 to 1 ratio of the fields for the two orientations to achieve such an overlap. This ratio determines the component H_\perp of the applied field $H \parallel \mathbf{a}$, which is due to c -axis misalignment of, or within, the film: it implies that an *average* of misalignment of the CuO_2 planes of 3.8° is required to explain the losses as in Ref. 6. Such a large average misalignment is unrealistic. Our x-ray-diffraction studies consistently show the HWHM of the rocking curve for $\text{Tl}_2\text{Ba}_2\text{CaCu}_2\text{O}_x$ films to be $< 0.4^\circ$, and in this case was only 0.2° for the (0010) peak. Using this value, the effect of any undulation of the CuO_2 planes is too small for H_\perp alone to explain the magnitude of the observed dissipation for $H \parallel \mathbf{a}$. The resistive transitions of the $\text{Bi}_2\text{Sr}_2\text{CaCu}_2\text{O}_x$ single crystals in magnetic fields are shown in Fig. 2, and we find a similar ratio of $\sim 10:1$ in effective fields. Here x-ray diffraction shows the HWHM of the rocking curve for $\text{Bi}_2\text{Sr}_2\text{CaCu}_2\text{O}_x$ single crystals is $< 0.6^\circ$ for the (0010) peak. Rough extrapolation of the other experimental results^{12,13} on $\text{Bi}_2\text{Sr}_2\text{CaCu}_2\text{O}_x$ films and single crystals with our ratios within factor of 2 or 3. Thus, in all cases, the values of H_\perp required by the model

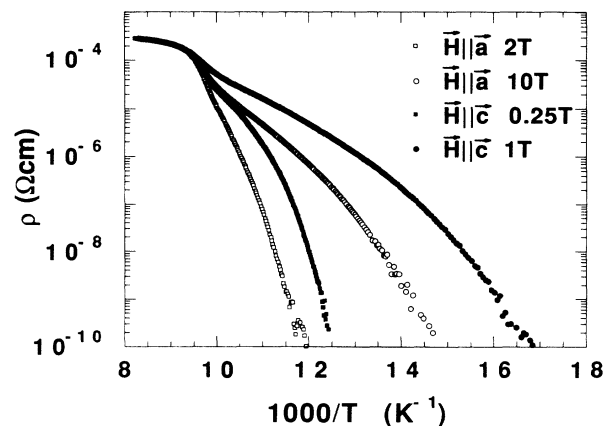


FIG. 1. The resistive tails of $\text{Tl}_2\text{Ba}_2\text{CaCu}_2\text{O}_x$ film for the applied field $H \perp \mathbf{a}$ and $H \parallel \mathbf{a}$ at measuring current density of 10 A/cm². These data are used to estimate the component of the applied field $H \parallel \mathbf{a}$, which is $\perp \mathbf{a}$, due to c -axis misalignment of, or within, the film, that is required to explain the losses as in Ref. 6.

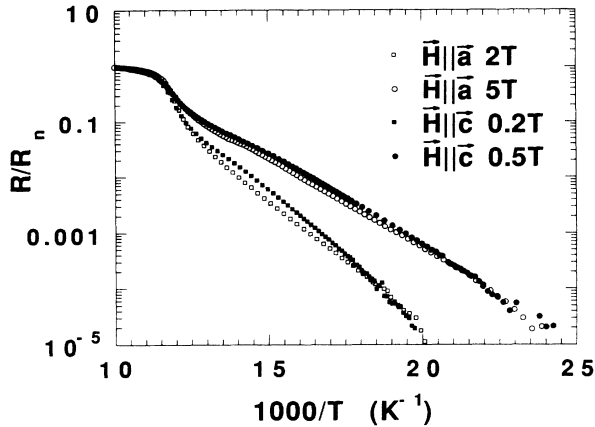


FIG. 2. Similar plot to Fig. 1 for the resistive tails of $\text{Bi}_2\text{Sr}_2\text{CaCu}_2\text{O}_x$ single crystal showing the scaling of field between $\mathbf{H}\parallel\mathbf{a}$ and $\mathbf{H}\parallel\mathbf{c}$ is a factor of 10.

of Ref. 6 are much too large to have resulted from the narrow distributions of c -axis misorientations or sample misalignments, and the suggestion⁶ that the macroscopic Lorentz-force independence of the resistive tails is a consequence of an unavoidable finite H_1 is in quantitative disagreement with these experiments.

In addition, the *shapes* of the “matched” curves in Figs. 1 and 2 for $\mathbf{H}\parallel\mathbf{a}$ and $\mathbf{H}\perp\mathbf{a}$ are not identical. In order to shed further light on this issue, the resistances for the $\text{Tl}_2\text{Ba}_2\text{CaCu}_2\text{O}_x$ films, shown in Figs. 3 and 4, for $\mathbf{H}\parallel\mathbf{a}$ and $\mathbf{H}\perp\mathbf{a}$, were fit to

$$\begin{aligned} \rho(T, H) &= \rho_0 \exp \left[\frac{-U(T, H)}{T} \right] \\ &= \rho_0 \exp \left[\frac{-U_0(H)(1-t)^q}{T} \right], \quad (1) \end{aligned}$$

where the activation energy $U(T, H)$ is assumed to have the form $U_0(H)(1-t)^q$, T is temperature and $t \equiv T/T_{c0}(H)$. Including $T_{c0}(H)$, this is a four-parameter

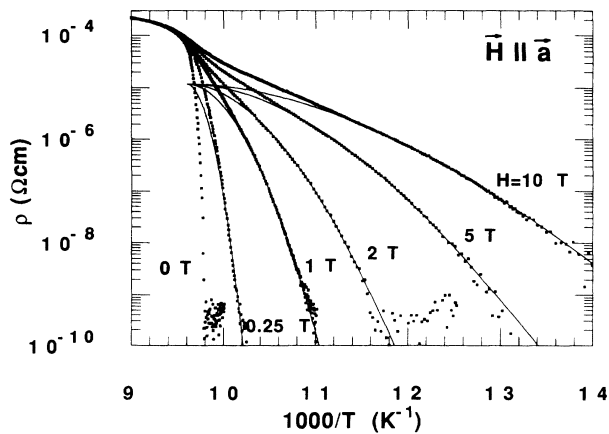


FIG. 3. Resistive transitions for $\mathbf{H}\parallel\mathbf{a}$ and $\mathbf{H}\perp\mathbf{a}$ showing the result of a one-parameter fit to Eq. (1). The parameters used are $\rho_0 = 1.2 \times 10^{-5} \Omega \text{cm}$, $T_{c0} = 104.2 \text{ K}$, and $q = 2$ while $U_0(H)$ is shown in Fig. 5.

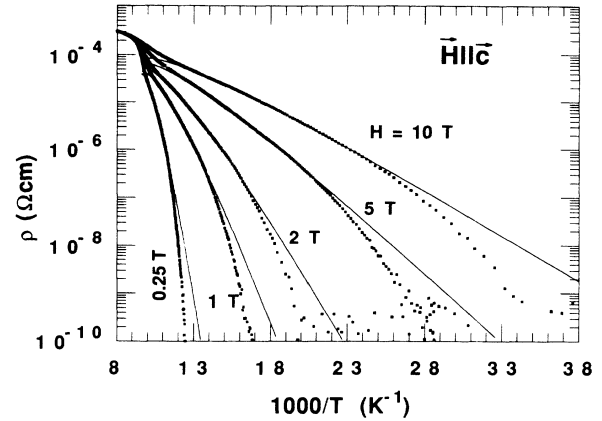


FIG. 4. Resistive transitions for $\mathbf{H}\parallel\mathbf{c}$ and $\mathbf{H}\perp\mathbf{c}$ showing the result of a two-parameter fit to Eq. (1). The parameters used are $q = 1.5$, $T_{c0}(0) = 104.2 \text{ K}$, and $\mu_0 H'_{c2} = 2 \text{ T/K}$, while $U_0(H)$ is shown in Fig. 5, and the increase of $\rho_0(H)$ with field is monotonic, but sublinear.

fit. The fitting procedure is complicated by the “double transitions,” found in Figs. 1–4, which are very reminiscent of resistive transitions for granular materials¹⁴ and two-dimensional Josephson junction¹⁵ or proximity-coupled¹⁶ superconducting arrays. In these cases, the superconducting grains or islands exhibit transitions at their critical temperature resulting in the initial resistance decrease, but not to zero resistance. These grains or islands then couple to each other with a supercurrent at a lower temperature. To avoid the ambiguity of the double transitions, all fitting of the resistivities excluded the higher-temperature transition.

For $\mathbf{H}\parallel\mathbf{a}$, we first established a fixed value for ρ_0 of $1.2 \times 10^{-5} \Omega \text{cm}$ from the highest field data (at 2–10 T), which is most sensitive to ρ_0 and least sensitive to $T_{c0}(H)$. It is clear that $\rho_0 < \rho_n(T_{c0})$, but that is necessary to properly account for the double transitions. We expect T_{c0} to be virtually unaffected by H because H_{c2} is so large, and a value of 104.2 K worked best. This is very close to the mean-field value of 104.6 K determined by fitting the resistance above T_{c0} to the two-dimensional fluctuation model.¹⁷ Finally to minimize the arbitrariness of the fit, we selected $q = 2$ and fitted over three orders of magnitude in fixed ranges of ρ between 10^{-9} to $10^{-5} \Omega \text{cm}$. The excellent agreement with experiments is shown in Fig. 3, and the only free parameter, $U_0(H)$, is shown in Fig. 5 and can be fit by

$$U_0(H) = 64500/H^{1.09}, \quad (2)$$

with H in T. Note that, because of the $(1-t)^q$ factor, U is considerably smaller than $U_0(H)$: it never exceeds $\sim 1000 \text{ K}$. In a second scheme, only ρ_0 was fixed, and the other three parameters were fit for all finite field values: this resulted in $q(H) = 1.53 - 1.65$, $T_{c0}(H) = 102.6 - 103.1 \text{ K}$ and $U_0(H)$ values about one-half the previous fit. The use of a larger fixed q of 2.4 led to reasonable fits, but with $T_{c0}(H)$ of 107 K for 2 T and 111 K for 10 T: These T_{c0} are too large and exhibit the wrong field dependence. Also, it would seem impossible to make a convincing fit

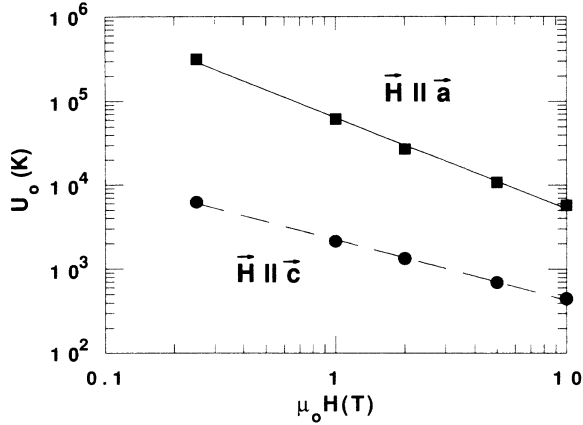


FIG. 5. The field dependence of $U_0(H)$ determined from the fits of Figs. 3 and 4 for $\mathbf{H}\parallel\mathbf{a}$ and $\mathbf{H}\parallel\mathbf{c}$. Note that, because of the $(1-t)^q$ factor, U is considerably smaller than $U_0(H)$: it never exceeds ~ 1000 K. The lines are fits described in the text.

to $q=1$, as was done for granular NbN films.⁸ Thus, using Eq. (1) and our $\rho(T, H)$ data, it is difficult to determine q more precisely than a range of about 1.5 to 2.

In the case of $\mathbf{H}\parallel\mathbf{a}$, the resistive transitions shown in Fig. 4 are significantly broader and T_{c0} is expected to depend on H . To minimize the parameters, we require an estimate of $T_{c0}(H)$. A lower limit for the upper critical-field slope, $H'_{c2} \equiv -dH_{c2}/dT$ at T_{c0} , of 1 T/K was obtained from the midpoints of the resistive transitions of $\text{Tl}_2\text{Ba}_2\text{CaCu}_2\text{O}_x$ films.⁹ Magnetization measurements, which give the thermodynamic $H_{c2}(T)$ and hence $T_{c0}(H)$, have not been reported for $\text{Tl}_2\text{Ba}_2\text{CaCu}_2\text{O}_x$, but for $\text{YBa}_2\text{Cu}_3\text{O}_7$ a value of ~ 2 T/K is found¹⁸ and this will be used together with $T_{c0}(0)=104.2$ K from above. Presuming first that the mechanism for $\mathbf{H}\parallel\mathbf{a}$ is the same as for $\mathbf{H}\parallel\mathbf{a}$, we set $\rho_0=1.2\times 10^{-5}\Omega\text{cm}$ and fitted again over three orders of magnitude in fixed ranges of ρ between 10^{-9} to $10^{-5}\Omega\text{cm}$. However, we found that all fits of Eq. (1) showed unreasonably large deviations with experiment for a fixed $q\leq 2$. If q was not fixed, the quality of the fits was close to that obtained for $\mathbf{H}\parallel\mathbf{a}$, with a peak dependence on $\mu_0 H'_{c2}$ from 0.5 to 4 T/K. The best fits, which used $\mu_0 H'_{c2}=2$ T/K, resulted in $q\sim 2.7$ for low fields, but larger values at the highest fields (e.g., $q=4.4$ at 10 T). The $U_0(H)$ is about 10% of the values found for $\mathbf{H}\parallel\mathbf{a}$. (Note that these values of $U_0(H)$ are *not* the ones shown in Fig. 5.) Fixing q at 2.4 and leaving $T_{c0}(H)$ free resulted in excellent agreement, but with $\mu_0 H'_{c2}=0.36$ T, which is too small based on the midpoints of the resistive transitions.⁹

From the above fitting, it is clear that a simple scaling⁶ of $\rho(T, H)$ at a large value of $\mathbf{H}\parallel\mathbf{a}$ to $\rho(T, H)$ at a smaller value of $\mathbf{H}\parallel\mathbf{a}$ will not work: although the effective field for the same U_0 is scaled by the same ratio ($\sim 10:1$), as was found for the previous qualitative comparison of $\rho(H, T)$, the exponent q is significantly different. For example, at $\mu_0 H\parallel\mathbf{a}=0.25\text{--}1$ T, $q=2.7\text{--}2.8$, while $q\leq 2$ for $\mu_0 H\parallel\mathbf{a}=10$ T. The field dependence of q and the unphysically large values (up to 4.4) point to possible problems

in the above fitting procedure for the case of $\mathbf{H}\parallel\mathbf{a}$. These inconsistencies in scaling indicate that the dominant mechanisms of dissipation might be different for the two field orientations with respect to the crystalline axes.

The large values of q were needed to fit the sharper drop of the experimental $\rho(T)$, below about $10^{-7}\Omega\text{cm}$, seen in Fig. 4 for $\mathbf{H}\parallel\mathbf{a}$. This sharper drop could result from a qualitative change in the dissipation. For example, if the resistive tails were predominantly due to thermally activated flux motion for $\mathbf{H}\parallel\mathbf{a}$, the sharp drop could reflect the onset of enhanced pinning. Flux motion is expected to be easier for $\mathbf{H}\parallel\mathbf{a}$ because the intrinsic pinning of the crystal structure is missing. To address this possibility, the transitions of Fig. 4 were fit to Eq. (1) between T_c and the sharp drop. If the mechanism of dissipation is different than for $\mathbf{H}\parallel\mathbf{a}$, then ρ_0 is not expected to be constant, nor the same value used above. The results of a two-parameter fit (q was fixed at 1.5, while ρ_0 and U_0 were varied) are shown in Fig. 4 as the solid lines. The agreement is excellent over the restricted range, but the fit clearly requires another explanation for low temperatures in Fig. 4. The values of $U_0(H)$, shown in Fig. 5, can be fit to $2200/H$.^{0.71}, while the increase of $\rho_0(H)$ with field was monotonic, but sublinear. Since the present paper is concerned with the Lorentz-force independence for $\mathbf{H}\parallel\mathbf{a}$, the data for $\mathbf{H}\parallel\mathbf{a}$ will be discussed elsewhere.

Finally, the resistive tails were measured as a function of current in films of $\text{Tl}_2\text{Ba}_2\text{CaCu}_2\text{O}_x$. For $\mu_0 H\parallel\mathbf{a}=1$ T, the resistive tails for current densities, J , of 10 A/cm² and 1000 A/cm² are shown in Fig. 6 for both field orientations *with respect to the current*: The minor differences in resistivities between $\mathbf{H}\perp\mathbf{I}$ and $\mathbf{H}\parallel\mathbf{I}$ are most likely due to thermal cycling upon remounting the sample. However, the data at higher current densities clearly demonstrate that the lack of a macroscopic Lorentz-force dependence does not depend on J .

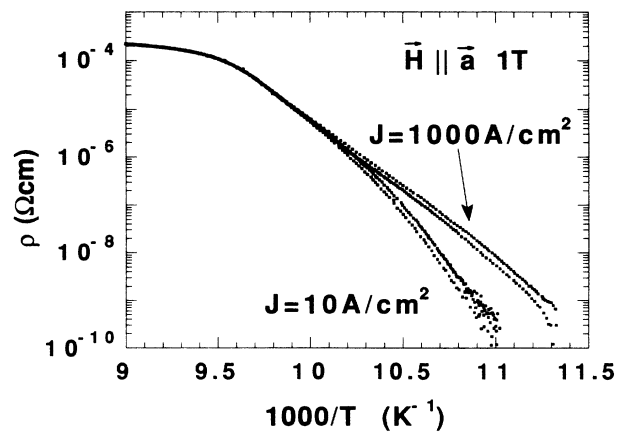


FIG. 6. The resistive tails at a 1 T field for $\mathbf{H}\parallel\mathbf{a}$ for measuring current densities of 10 and 1000 A/cm² which are perpendicular (slightly larger ρ) and parallel to the field. The differences in the tails between the two current directions are ascribed to thermal cycling between measurements and are shown here to be unaffected by increasing the measuring current density.

B. Current-voltage characteristics, $I(V)$

The $I(V)$ near the resistive tail region were measured for all orientations of field and current available. For $\mathbf{H}\parallel\mathbf{a}$, there were only minor differences between $\mathbf{H}\perp\mathbf{I}$ and $\mathbf{H}\parallel\mathbf{I}$: The $I(V)$ were parallel on a log-log plot, but shifted in current by about 10% for all T as shown in Fig. 7. Figure 6 shows similar shifts in the resistive tails which were ascribed to thermal cycling of the sample and the same is likely here, thus indicating no Lorentz-force dependence. For $\mathbf{H}\perp\mathbf{a}$, the $I(V)$ are shown in Fig. 8 for a temperature range from 24 to 46 K in a 5 T field. The overall shapes show a similar trend to $\text{YBa}_2\text{Cu}_3\text{O}_7$ films¹⁹ for $\mathbf{H}\perp\mathbf{a}$, but we do not find a pure power law in the $I(V)$ at any temperature nor the scaling necessary to fit to the vortex glass model,²⁰ perhaps because $\text{Ti}_2\text{Ba}_2\text{CaCu}_2\text{O}_x$ is more two dimensional.

At the lowest temperatures shown, the $I(V)$ show a characteristically different shape, as noted previously,¹⁹ exhibiting negative curvature. This negative curvature allows a natural definition of I_c without requiring an ambiguous voltage criterion. (At room temperature even a carbon radio resistor exhibits a finite I_c based on voltage criterion!) It is important to recognize that the $I(V)$ therefore provide the necessary clue to determine when J_c measurements, made with an appropriate voltage criterion, indicate the dramatic onset of dissipation or just reflect the continuing broadening of the resistive transition. Such negative curvature in a log-log plot of $I(V)$ occurs only when the resistance is saturating to the normal-state value near I_c : this can be shown for Josephson junctions and must be true for flux creep. The Anderson-Kim model²¹ ignores the normal-state limit of resistance and predicts only an exponential increase of V with I . However, Tinkham's reformulation^{22,23} includes this saturation in the same manner as for Josephson junctions.

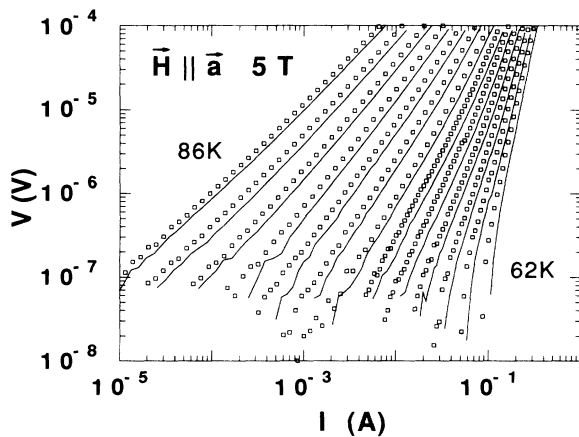


FIG. 7. For $\mathbf{H}\parallel\mathbf{a}$ of 5 T, the $I(V)$ show only minor differences between $\mathbf{H}\parallel\mathbf{I}$ (lines) and $\mathbf{H}\perp\mathbf{I}$ (open squares) that are similar to shifts in the resistive tails which were ascribed to thermal cycling the sample. The same is likely here, thus indicating no Lorentz-force dependence of $I(V)$. The temperature step between successive curves is ~ 2 K.

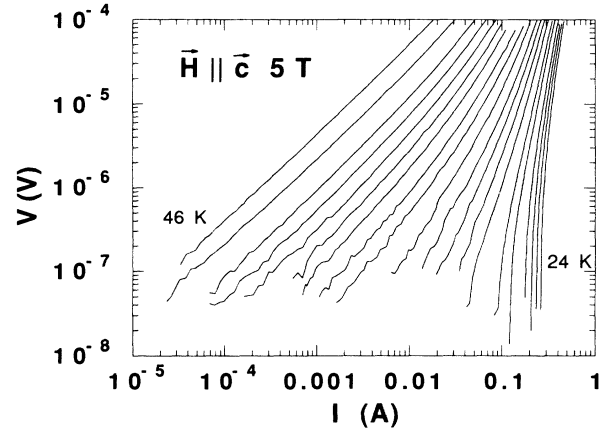


FIG. 8. Current-voltage characteristics for $\mathbf{H}\perp\mathbf{a}$ in a 5 T field between 24 and 46 K. The temperature step between successive curves is ~ 1 K except for the two highest temperatures.

C. Critical current density, J_c

Measurements of J_c can always be related to the resistive tails: For a given field, the temperature, T , at which the resistance (or more commonly, the voltage) of the tail drops below some arbitrary value defines $J_c(H, T)$ as equal to the measuring current density. Although the results of Fig. 6 could be extended to higher current density to determine J_c , a voltage criterion at fixed H and T is more convenient, and the customary $1 \mu\text{V}/\text{cm}$ was used to define J_c for $\mathbf{H}\perp\mathbf{a}$ and $\mathbf{H}\parallel\mathbf{a}$. For $\mathbf{H}\parallel\mathbf{a}$, these data are shown in Fig. 9, superimposed for both orientations of H with respect to current: there is no evidence for a macroscopic Lorentz-force dependence from 4.2 to 93 K in fields up to 10 T. The macroscopic Lorentz-force independence of J_c is remarkable when compared to the dependence in ordinary type-II superconductors which show²⁴ an anisotropy in J_c of 20–100 for the same geometry. In Nb_3Sn , furthermore, the inverse of the critical current varies in accordance with the Lorentz-force model as $\sin\theta$, where θ is the angle between H and I , except for a narrow region near $\theta=0$ where other mechanisms⁵ limit J_c .

From the above discussion of the $I(V)$, it is the negative curvature at low voltages which indicates the onset of dissipation at a true "critical" value of current. Since the $J_c(H, T)$ shown in Fig. 9 are determined from a voltage criterion, a value is always measured whether the $I(V)$ exhibits negative curvature or just represents a continuous spreading of the resistive transition. Thus, we display (see also Ref. 25) the onset of negative curvature of $I(V)$ in Fig. 9 with the solid line (from data accumulated for $\mu_0 H = 2$ and 5 T), and point out that it corresponds closely to the rapid decreases of J_c with field, found at the higher temperatures. Figure 10 shows the temperature dependence of J_c , using only values for which the $I(V)$ exhibit negative curvature, and the best fits are for an exponent of $(1-t)$ which is ~ 2 . The dependence of

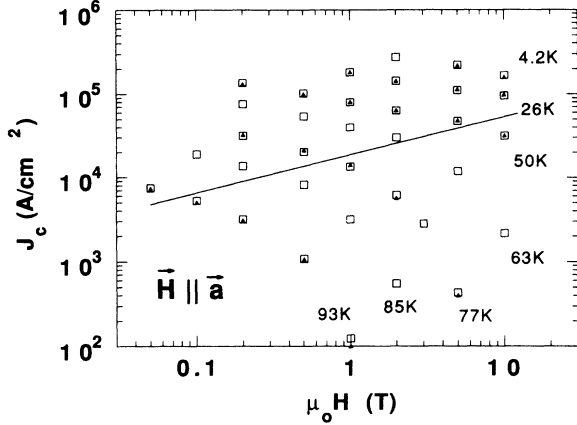


FIG. 9. The critical current densities, J_c , for $\mathbf{H}\parallel\mathbf{I}$ (open squares) and $\mathbf{H}\parallel\mathbf{I}$ (solid triangles) vs magnetic field at the temperatures indicated for $\mathbf{H}\parallel\mathbf{a}$. These clearly indicate no macroscopic Lorentz-force dependence of J_c . The $I(V)$ for data above the solid line show negative curvature.

$J_c(H, T)$ can be parametrized as

$$J_c(H, T) = \frac{300\,000 \text{ A/cm}^2}{H^{0.24}} \left[1 - \frac{T}{T_{c0}} \right]^2, \quad (3)$$

for which we forced the exponent to be 2 and $T_{c0} = 104.2 \text{ K}$.

Because of the film geometry, J_c for $\mathbf{H}\perp\mathbf{a}$ can only be measured with $\mathbf{H}\perp\mathbf{I}$, and these are plotted in Fig. 11, in which the solid line again delineates the appearance of negative curvature in the $I(V)$ at lower temperatures. For the lowest temperatures, the field dependence of J_c is consistent with $H^{-0.24}$ as in Eq. (3), but the scatter in the data over the limited region exhibiting negative curvature prevented an accurate determination of the temperature dependence. When J_c with negative curvature in $I(V)$ are compared for $\mathbf{H}\parallel\mathbf{a}$ and $\mathbf{H}\perp\mathbf{a}$, a ratio of $\sim 10\text{--}15:1$ is again found for the effectiveness of the magnetic field.

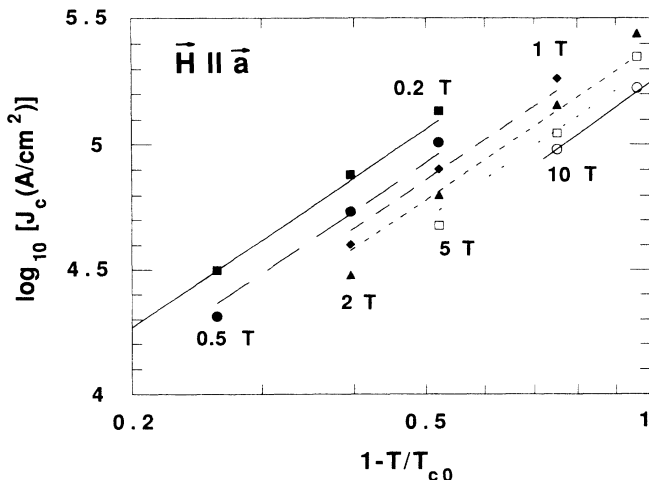


FIG. 10. The temperature dependence of J_c at the various indicated field values.

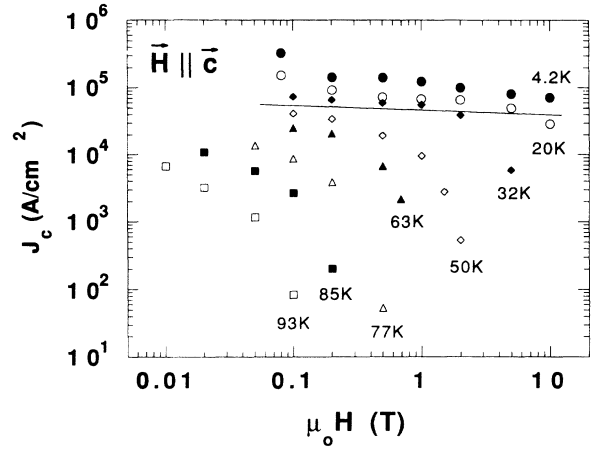


FIG. 11. Same as Fig. 9 except $\mathbf{H}\perp\mathbf{a}$ and only $\mathbf{H}\perp\mathbf{I}$ is experimentally accessible.

Using the same argument given for the tails, it is evident that the formation of a vortex lattice related⁶ to H_{\perp} is insufficient to explain the ratio of J_c between $\mathbf{H}\perp\mathbf{a}$ and $\mathbf{H}\parallel\mathbf{a}$ in these $\text{Tl}_2\text{Ba}_2\text{CaCu}_2\text{O}_x$ films.

D. Summary

All the transport measurements reported in this paper, ρ , $I(V)$ and J_c , as a function of temperature and $\mathbf{H}\parallel\mathbf{a}$, show little or no dependence on the macroscopic Lorentz force. Even if the small difference shown in Figs. 6 and 7 are real, the broadened resistive transitions, $I(V)$ and J_c for $\mathbf{H}\parallel\mathbf{I}$ are so similar to $\mathbf{H}\perp\mathbf{I}$ that the Lorentz force is at most a perturbation. In addition, the suggestion⁶ that vortices in the CuO_2 planes, due to a small misalignment of $\mathbf{H}\parallel\mathbf{a}$, are responsible for these effects has been shown to consistently require a field component perpendicular to \mathbf{a} which is significantly larger than is reasonable, based on the measured alignment of the samples and crystal axes. The measurements with $\mathbf{H}\parallel\mathbf{c}$ leave open the possibility that a different mechanism than that for $\mathbf{H}\parallel\mathbf{a}$ is partially or totally involved.

IV. JOSEPHSON-COUPLING MODEL

The independence of the above data for $\mathbf{H}\parallel\mathbf{a}$ on the Lorentz force implies that the dominant dissipation mechanism is something other than flux motion. We consider fluctuations in Josephson junctions and show that they are consistent with the broadened resistive transitions and the lack of Lorentz-force dependence on all properties reported in this paper. Such a model has satisfactorily explained similar results in granular NbN films,⁸ and J_c measurements in granular NbN/AlN multilayers have shown²⁶ a crossover between flux flow and Josephson coupling. In these cases, traditional models for the Josephson critical current²⁷ and dissipation²⁸ were used, and the junctions occurred laterally in the film plane, across insulating boundaries between the columnar grains.²⁹ In making a connection, it should be emphasized that the measurements on HTS were made on single crystal or very large-grained thin films which do

not have obvious structural defects to produce Josephson junctions as do the granular NbN films and NbN/AlN multilayers. However, Larbalestier and Daeumling³⁰ have recently proposed a model of *field-induced* granularity in single crystals of YBa₂Cu₃O₇ which convincingly explains their magnetization data. In this model, the field suppresses the superconductivity in regions that are already weakened by either point or extended microscopic defects, which are not seen in conventional analyses of these crystals. Field-enhanced J_c have been previously measured in conventional superconductors with second-phase precipitates.³¹ Phillips³² has also recently concluded that YBa₂Cu₃O₇ exhibits “a complex micromorphology which is not revealed by ordinary diffraction experiments.” Either of these models^{30,32} could lead to weak limits or Josephson coupled regions or “grains,” even in the absence of obvious structural defects.

While the junctions could have their origins in the above models of complex micromorphology³² or *field-induced* granularity,³⁰ due to unspecified point or extended microscopic defects (oxygen vacancies were postulated³⁰ for single crystals of YBa₂Cu₃O₇), another possible origin is Josephson coupling between superconducting layers,³³ in this case the intrinsic CuO₂ planes. These interlayer junctions play a role in transport properties if current flow is not confined to individual CuO₂ planes, but most cross to other planes by Josephson tunneling. The probability of microscopic defects or fluctuations blocking the current flow is drastically increased in the two-dimensional (2D) CuO₂ planes compared to 3D superconductors. Whatever the origin of junctions in HTS is, we find two common features of all these materials (granular NbN and NbN/AlN multilayers and HTS, like Tl₂Ba₂CaCu₂O_x): the Lorentz-force independence of the resistive tails and internal Josephson junctions.

It is of interest to further consider the intrinsic interlayer Josephson junctions, since *they give a natural explanation of the variation of the broadened resistive transitions with HTS material.* The layers are so weakly coupled in Tl₂Ba₂CaCu₂O_x that each layer behaves almost independently. Evidence for this comes from: the huge anisotropy of H_{c2} with the consequent extremely short Ginzburg-Landau coherence length along the c axis;⁹ torque magnetization;¹⁰ and two-dimensional fluctuations.¹⁷ For such weak coupling, thermal fluctuations can be a dominant limiting factor on the Josephson coupling and hence transport properties of the system, such as resistive losses. By comparison, the coupling between layers is inherently stronger in YBa₂Cu₃O₇ (the electron effective-mass ratio is ~ 25 compared to $\sim 10^4$ in Tl₂Ba₂CaCu₂O_x in Ref. 10) and therefore the relative effect of fluctuations will be significantly reduced. From these considerations, we can understand the observation in³⁴ YBa₂Cu₃O₇ (for $\mathbf{H} \parallel \mathbf{a}$) of dissipation by flux motion *together with the large Lorentz-force-independent background.* The relative strengths of interlayer Josephson coupling can explain how the Josephson fluctuation mechanism could be comparable in magnitude to flux motion in YBa₂Cu₃O₇, but dominate transport in Tl₂Ba₂CaCu₂O_x.

Note that since the Tl₂Ba₂CaCu₂O_x films are polycrys-

talline, albeit with a high degree of c -axis orientation, Josephson coupling could be between the grains. However, similar results³ obtained on single crystals of Tl₂Ba₂CaCu₂O_x suggest that the Lorentz-force-independent characteristics are not a result of thin-film grains.

V. COMPARISON WITH JOSEPHSON COUPLING AND FLUX FLOW

It is clear that the absence of the Lorentz force in all the measurements reported in this paper favors that a mechanism other than flux-flow controls the dissipation in Tl₂Ba₂CaCu₂O_x films for $\mathbf{H} \parallel \mathbf{a}$. Lorentz-free independent dissipation is compatible with a Josephson-coupling model.⁸ In the following, the experimental results of this paper for $\mathbf{H} \parallel \mathbf{a}$ are analyzed within the Josephson-coupling and flux-flow models of the dissipation.

A. Resistive transitions

Here we consider the consistency of the parameters of the fit to Eq. (1) for $\mathbf{H} \parallel \mathbf{a}$ with these models. In classical Josephson junctions of the superconductor-insulator-superconductor (SIS) type, U is given²⁸ in zero field as

$$U = \hbar I_{cj} / ek_B, \quad (4)$$

where the Josephson critical current, I_{cj} , also depends²⁷ on the magnitude of the superconducting order parameter, ψ , or the energy gap, $\Delta(T)$, such that

$$I_{cj}(T) = \frac{\pi \Delta(T)}{2eR_N} \tanh \left[\frac{\Delta(T)}{2k_B T} \right], \quad (5)$$

which goes as $(1-t)$ near T_{c0} , and the corresponding low-temperature limit is $I_{cj}(0) \sim \pi \Delta(0) / 2eR_N$. Here R_N is the junction resistance above T_{c0} . An extension of the model to finite fields⁸ relied on the uniformity of B due to the penetration depth being larger than the other relevant lengths, as it is in HTS, and used the Abrikosov solution for the vortex lattice for the field dependence of $\langle \psi^2 \rangle$ as $1 - B / \mu_0 H_{c2}$. Combining these for T near T_{c0} :

$$U = 2.56 \pi T_{c0} R_0 / R_N (1 - B / \mu_0 H_{c2}) (1-t), \quad (6)$$

where $R_0 \equiv \hbar / e^2 = 4114 \Omega$.

The field and temperature dependence of Eq. (6) was confirmed by measurements in granular NbN films,⁸ but the temperature dependence of Eq. (6) is in conflict with the fits of Fig. 3 for which $q = 1.5$ to 2. This conflict can be resolved by recent measurements³⁵ on individual grain-boundary junctions in YBa₂Cu₃O₇ showing $I_c \sim (1-t)^2$. These have been interpreted as SIS in which the boundary conditions of Deutscher and Müller³⁶ are applied to the order parameter at the insulator boundary: thus³⁷

$$U = 2.56 \pi T_{c0} [a / \xi(0)]^2 R_0 / R_N (1-t)^2, \quad (7)$$

where $\xi = \xi(0) / \sqrt{1-t}$ is the superconducting coherence length and a is the lattice constant.

Superconductor-normal-superconductor (SNS) proximity junctions^{16,38} are another possibility for the Joseph-

son coupling. The temperature and field dependences for clean N layers has been summarized³⁹ as

$$U(T, H) \sim \hbar I_c(t) e k_B \sim T_{c0} (R_0/R_N) (1-t)^2 \exp(-d_N \alpha t), \quad (8)$$

where d_N is the N layer thickness, $\alpha = \alpha_0 \sqrt{1 + sB/T}$, $\alpha_0 = 2\sqrt{3\pi} k_B T_{c0} / \hbar v_F$, v_F is the electron Fermi velocity and s is proportional to the electron diffusivity in the normal-metal layer. The exponential dependence of U or J_c on \sqrt{B} or t is only seen³⁹ in low-temperature superconductors well below T_{c0} : its absence here from the experimental data at any temperature could be used to rule out SNS junctions, but a crossover to another mechanism which limits J_c at low temperatures is also possible.

The flux-creep model of Tinkham²² predicts $k_B U(T, H) \sim \mu_0 H_c^2 V_a$, where the superconducting condensation energy is multiplied by the volume triggering the flux jump, $V_a \sim \xi \Phi_0 / B$. Hence, $U(T, H) \sim (1-t)^{1.5} / B$, which is consistent with an acceptable fit of the data of Fig. 3 for $\mathbf{H} \parallel \mathbf{a}$. However, the factor of ξ results from the length *along the flux lines* of the region triggering the flux jump. For the very weak coupling between CuO_2 planes in $\text{Ti}_2\text{Ba}_2\text{CaCu}_2\text{O}_x$, there are no continuous flux lines between these planes and the flux cores in each CuO_2 plane act independently. Therefore, for any H_1 resulting from misalignment, perhaps ξ should be replaced with a temperature-independent length the order of the CuO_2 planar spacing, and then $U(T, H) \sim (1-t)^2 / B$. Thus the flux-creep model fits the experimental result of $U(T, H) \sim (1-t)^2 / B$ for $\mathbf{H} \parallel \mathbf{a}$, but both models are consistent with the temperature dependence.

B. Current-voltage characteristics

Both the Josephson-coupling model^{27,28} and the Anderson-Kim flux-creep theory²¹ predict a linear voltage response at low currents followed by positive curvature of V as I increases. At higher currents, the Josephson model predicts negative curvature as the junction resistance approaches its normal-state value, while the Anderson-Kim model, which ignores the normal-state limit of resistance, predicts only an exponential increase of V with I (which implies strictly positive curvature on the $\log(V)$ - $\log(I)$ plots of Figs. 7 and 8). A more complete flux-creep model must include saturation at the normal-state resistance, but no detailed theoretical predictions are known to the authors. It is also hard to distinguish between the predictions of these models below saturation, given some freedom of parameter choices. Therefore, the best we can do at present is say that our $I(V)$ data do not confirm, nor rule out, either model.

C. Critical current density

In the Josephson-coupling model [see Eq. (4)], the critical current, $I_c(H, T)$, is strictly proportional to U . This has been demonstrated⁸ for granular NbN, in which the columnar grains were assumed to be on a square lattice, so the junctions between each pair of grains had an area

$\sim da_0$, where d is the film thickness and a_0 the average grain diameter. Thus, $I_c(H, T)$ should be equal to $da_0 J_c(H, T)$, and U_0 and J_c were shown⁸ to have the same field dependence of $1 - B/\mu_0 H_{c2}$. These measurements also verified the $1-t$ dependence of U and the inverse dependence of I_c on R_N , the normal resistance of the junctions. In this granular model, R_N could be approximated by ρ_N/d , because the junction resistances dominated ρ_N , the normal-state resistivity of the film along its length. Similar considerations apply for the SIS model of Ref. 35, although the temperature dependences of U and J_c are then $(1-t)^2$, and the SNS model, in which U and J_c are also $\sim (1-t)^2$ near T_{c0} , but exhibit exponential dependences at low temperature and high field. The dependence on normal-state resistance is also complicated by the exponential dependence³⁸ on d_N .

The modified flux-creep model^{22,23} derives $J_c \sim U / BV_d L$, where V_d is the volume of the minimum region triggering an activated event and L is the typical distance moved. The interpretation of results on $\text{YBa}_2\text{Cu}_3\text{O}_7$ films²³ led to an evaluation of V_d and L leading to $J_c \sim (1-t)U$. This result is the main difference with the Josephson-coupling models, for which $J_c \sim U$. If we make the reasonable assumption that the length of the flux lines is restricted to the CuO_2 planar spacing rather than proportional to $\xi(T)$ (as assumed above to fit the experimental temperature dependence of U), then $J_c \sim (1-t)^3 / B$. This is clearly too strong a dependence for both temperature and field when compared to our measurements for $\mathbf{H} \parallel \mathbf{a}$, which are summarized in Eq. (5).

D. Summary

The above comparisons are not sufficiently incisive to rule out any mechanism considered for dissipation in $\text{Ti}_2\text{Ba}_2\text{CaCu}_2\text{O}_x$, for $\mathbf{H} \parallel \mathbf{a}$. *The main difference in the models is the ratio J_c/U* : it is temperature independent in the Josephson-coupling model, but proportional to $1-t$ for the modified flux-creep model.^{22,23} Our results indicate that the temperature dependences of J_c and U are the same, favoring the Josephson-coupling model. However, it would be useful to have some specific predictions about the parameters for the flux-creep model. In addition, it is possible that the dominant dissipation mechanisms for J_c and the resistive tails (through U) are different: This is unappealing since they both exhibit the same Lorentz-force independence, but, e.g., they could be inter- and intra-granular Josephson junctions since J_c was not checked in the single-crystal work.³ The flux-creep model fits the experimental result for $U(T, H)$, but predicts much stronger temperature and field dependences for J_c than are found. The SIS and SNS Josephson models are consistent with the temperature dependences of $U(T, H)$ and $J_c(T, H)$, and are closer to the weak-field dependence measured for J_c .

Both models are rather vague, and a better prediction for the field dependence of the Josephson-coupling model in the highly anisotropic HTS-like $\text{Ti}_2\text{Ba}_2\text{CaCu}_2\text{O}_x$ is still needed. Nonetheless, presuming that both J_c and U are limited by the same Josephson junctions, the different

field dependences of J_c and U , which is strictly proportional to I_c in the Josephson-coupling model, means that the relevant area of the junctions, A_j , must depend on field as $H^{-0.85}$. The magnitude of $A_j(H)$ is harder to assess since we cannot assume $I_c = J_c A_j$, as⁸ for the columnar grains of NbN, because the specific junction geometry is not known and it could be between CuO_2 planes.

VI. SUMMARY AND CONCLUSIONS

The universal lack of a Lorentz-force dependence¹⁻⁴ on dissipation in the highly anisotropic HTS-like $\text{Ti}_2\text{Ba}_2\text{CaCu}_2\text{O}_x$ for $\mathbf{H}\parallel\mathbf{a}$, as measured by the broadened resistive transitions, current-voltage characteristics and critical current densities, leads one to suspect that these may not be caused by flux motion. We have ruled out the suggestion⁶ that vortices in the CuO_2 planes, due to a small misalignment of $\mathbf{H}\parallel\mathbf{a}$, are responsible for this effect: such an explanation consistently required a field component perpendicular to \mathbf{a} which is significantly larger than is reasonable, based on the measured alignment of the samples and crystal axes.

As an alternative to flux motion, we consider a Josephson-coupling model (explained in detail in Secs. IV and V) which is consistent with the broadened resistive transitions and the lack of Lorentz-force dependence on all properties reported in this paper. A detailed comparison of the experimental data with the predictions of the Josephson-coupling and flux-flow models is made for $\mathbf{H}\parallel\mathbf{a}$. The main difference in the models is the ratio J_c/U : it is temperature independent in the Josephson-coupling model, but proportional to $1-t$ for the modified flux-creep model.^{22,23} Our results indicate that the temperature dependences of J_c and U are the same, favoring the Josephson-coupling model. Although it is possible that

the dominant dissipation mechanisms for J_c and the resistive tails (through U) are different, this is unappealing since they both exhibit the same Lorentz-force independence. The Josephson-coupling model is consistent with the temperature dependences of $U(T,H)$ and $J_c(T,H)$, and is better matched to the weak-field dependence measured for J_c . The flux-creep model fits the experimental result for $U(H)$, but predicts much stronger temperature and field dependences of J_c than are found. Although no definitive choice of model can be made, based on the T and H dependence of U and J_c , the Josephson-coupling model agrees at least as well as flux creep and is consistent with the Lorentz-force independence. Possible origins of Josephson junctions in high-quality films and single crystals are discussed.

Fitting the measurements for $\mathbf{H}\parallel\mathbf{c}$ requires sufficiently different parameters that it leaves open the possibility that a different mechanism than that for $\mathbf{H}\parallel\mathbf{a}$ is partially or totally involved. For example, flux motion is expected to be easier for $\mathbf{H}\parallel\mathbf{c}$ because the intrinsic pinning of the crystal structure is missing.

ACKNOWLEDGMENTS

The authors thank Dr. Donglu Shi for providing $\text{Bi}_2\text{Sr}_2\text{CaCu}_2\text{O}_x$ single crystals and J. Stein for assistance with the data acquisition. This work was supported by the U.S. Department of Energy, Division of Basic Energy Sciences—Materials Sciences, under Contract No. W-31-109-ENG-38 and the National Science Foundation—Office of Science and Technology Centers under Contracts No. STC-8809854 D. M. M., Science and Technology Center for Superconductivity—University of Illinois of Urbana-Champaign. D. M. M. acknowledges support from the Division of Educational Programs, Argonne National Laboratory.

- ¹Y. Iye, S. Nakamura, and T. Tamegai, *Physica C* **159**, 433 (1989); K. Kitazawa, S. Kambe, M. Naito, I. Tanaka, and H. Kojima, *Jpn. J. Appl. Phys.* **28**, L555 (1989); S. Kambe, M. Naito, K. Kitazawa, I. Tanaka, and H. Kojima, *Physica C* **160**, 243 (1989).
²R. C. Budhani, D. O. Welch, M. Suenaga, and R. L. Sabatini, *Phys. Rev. Lett.* **64**, 1666 (1990).
³H. Iwasaki, N. Kobayashi, M. Kikuchi, S. Nakajima, T. Kajitani, Y. Syono, and Y. Muto, *Physica C* **159**, 301 (1989).
⁴K. C. Woo, K. E. Gray, R. T. Kampwirth, J. H. Kang, S. J. Stein, R. East, and D. M. McKay, *Phys. Rev. Lett.* **63**, 1877 (1989).
⁵J. R. Clem, *Phys. Rev. B* **26**, 2463 (1982).
⁶P. H. Kes, J. Aarts, V. M. Vinokur, and C. J. van der Beek, *Phys. Rev. Lett.* **64**, 1063 (1990).
⁷D. E. Farrell (private communication).
⁸D. H. Kim, K. E. Gray, R. T. Kampwirth, K. C. Woo, D. M. McKay, and J. Stein, *Phys. Rev. B* **41**, 11 642 (1990).
⁹J. H. Kang, K. E. Gray, R. T. Kampwirth, and D. W. Day, *Appl. Phys. Lett.* **53**, 2560 (1988).
¹⁰K. E. Gray, R. T. Kampwirth, and D. E. Farrell, *Phys. Rev. B* **41**, 819 (1990).
¹¹Donglu Shi, Ming Tang, Y. C. Chang, P. Z. Ziang, K. Vande-

- voort, B. Malecki, and D. J. Lam, *Appl. Phys. Lett.* **54**, 2358 (1989).
¹²T. T. M. Palstra, B. Batlogg, L. F. Schneemeyer, and J. V. Waszczak, *Phys. Rev. Lett.* **61**, 1662 (1988).
¹³Y. Iye, in *Strong Correlation and Superconductivity*, Vol. 89 of *Springer Series in Solid State Sciences*, edited by H. Fukuyama, S. Maekawa, and A. P. Malozemoff (Springer-Verlag, Berlin, 1989), p. 213.
¹⁴S. A. Wolf, D. U. Gubser, W. W. Fuller, J. C. Garland, and R. S. Newrock, *Phys. Rev. Lett.* **47**, 1071 (1981).
¹⁵R. F. Voss and R. A. Webb, *Phys. Rev.* **25**, 3446 (1982).
¹⁶D. J. Resnick, J. C. Garland, J. T. Boyd, S. Shoemaker, and R. S. Newrock, *Phys. Rev. Lett.* **47**, 1542 (1981); D. W. Abraham, C. J. Lobb, M. Tinkham, and T. M. Klapwijk, *Phys. Rev.* **26**, 5268 (1982).
¹⁷D. H. Kim, A. M. Goldman, J. H. Kang, R. T. Kampwirth, and K. E. Gray, *Phys. Rev. B* **39**, 12 275 (1989).
¹⁸U. Welp, W. K. Kwok, G. W. Crabtree, K. G. Vandervoort, and J. Z. Liu, *Phys. Rev. Lett.* **62**, 1908 (1989).
¹⁹R. H. Koch, V. Foglietti, W. J. Gallagher, G. Koren, A. Gupta, and M. P. A. Fisher, *Phys. Rev. Lett.* **63**, 1511 (1989).
²⁰M. P. A. Fisher, *Phys. Rev. Lett.* **62**, 1415 (1989).
²¹P. W. Anderson, *Phys. Rev. Lett.* **9**, 309 (1962); P. W. Ander-

- son and Y. B. Kim, *Rev. Mod. Phys.* **36**, 39 (1964).
- ²²M. Tinkham, *Phys. Rev. Lett.* **61**, 1658 (1988).
- ²³J. D. Hettinger, A. G. Swanson, W. J. Skocpol, J. S. Brooks, J. M. Graybeal, P. M. Mankiewich, R. E. Howard, B. L. Straughn, and E. G. Burkhardt, *Phys. Rev. Lett.* **62**, 2044 (1989).
- ²⁴G. D. Cody and G. W. Cullen, *RCA Rev.* **25**, 466 (1964); J. W. Heaton and A. C. Rose-Innes, *Cryogenics* **4**, 85 (1964); V. R. Karasik and V. G. Vereshchagin, *Zh. Eksp. Teor. Fiz.* **59**, 36 (1970) [*Sov. Phys.—JETP* **32**, 20 (1971)].
- ²⁵M. A. Stan, S. A. Alterovitz, D. Ignjatovic, K. B. Bhasin, G. C. Valco, and N. J. Rohrer, *Physica C* **162–164**, 365 (1989).
- ²⁶K. E. Gray, R. T. Kampwirth, D. J. Miller, J. M. Murduck, D. Hampshire, R. Herzog, and H. W. Weber (unpublished).
- ²⁷P. W. Anderson (unpublished); V. Ambegaokar and A. Bartakoff, *Phys. Rev. Lett.* **10**, 486 (1963).
- ²⁸V. Ambegaokar and B. I. Halperin, *Phys. Rev. Lett.* **22**, 1364 (1969).
- ²⁹H. L. Ho, R. T. Kampwirth, K. E. Gray, D. W. Capone II, and L. S. Chumbley, *Ultramicroscopy* **22**, 297 (1987).
- ³⁰M. Daeumling, J. M. Seuntjens, and D. C. Larbalestier, *Nature (London)* **346**, 332 (1990).
- ³¹J. D. Livingston, *Appl. Phys. Lett.* **8**, 319 (1966); K. E. Gray, R. T. Kampwirth, J. F. Zasadzinski, and S. P. Ducharme, *J. Phys. F* **13**, 405 (1983).
- ³²J. C. Phillips, *Phys. Rev. Lett.* **64**, 1605 (1990).
- ³³W. E. Lawrence and S. Doniach, in *Proceedings of the 12th International Conference on Low Temperature Physics*, edited by E. Kanda (Academic Press of Japan, Kyoto, 1971), p. 361.
- ³⁴W. K. Kwok, U. Welp, G. W. Crabtree, K. G. Vandervoort, R. Hulscher, and J. Z. Liu, *Phys. Rev. Lett.* **64**, 966 (1990).
- ³⁵R. Gross, P. Chaudhari, D. Dimos, A. Gupta, and G. Koren, *Phys. Rev. Lett.* **64**, 228 (1990).
- ³⁶D. Deutscher and K. A. Müller, *Phys. Rev. Lett.* **59**, 1745 (1987).
- ³⁷An apparent typographical error in Ref. 35 shows $\Delta_i \sim \Delta_0 \xi(0)/a$ instead of $\Delta_0 a / \xi(0)$, as in Ref. 36.
- ³⁸P. G. de Gennes, *Rev. Mod. Phys.* **36**, 225 (1964).
- ³⁹T. Y. Hsiang and D. K. Finnemore, *Phys. Rev. B* **22**, 154 (1980).